CHAPTER 4
PREPARATION OF NANO-SIZED CeO_2 BY DIFFERENT MICROEMULSION METHODS[*]

4.1 Introduction

During the past decade, cerium oxide has been commonly reported to apply as catalyst in a wide variety of reactions involving oxidation or partial oxidation of hydrocarbons. A high oxygen mobility (redox property), high oxygen storage capacity, strong interaction with the supported metal (strong metal–support interaction), and the modifiable ability render this material very interesting for catalysis. Recently, the reactivity toward methane steam reforming with high resistance toward carbon deposition over ceria has been observed. Unfortunately, the steam reforming reactivity over CeO_2 was too low compared to the conventional metallic catalysts. This is mainly due to its low specific surface area, and its high sintering rate at high temperature [48]. In order to minimize the weakness of CeO_2 in terms of its low specific surface area, CeO_2 prepared by microemulsion method in this work should have the high surface area and small particle size.

According to the investigation of He *et al.* [6], it was found that CeO_2 was prepared by coupling route of homogenous precipitation with microemulsion showed high surface area and the nanometer particle size. The study of surfactants type on the average particle size showed that anionic surfactant had the smallest particle size. Hadi and Yaacob [49] studied the preparation of nanocrystalline CeO_2 by mechanochemical and W/O microemulsion. It was found that CeO_2 prepared by microemulsion was more stable than those prepared by mechanochemical method against the effect of heat treatment and the sample has higher specific surface area which was non-porous. In 2008, Sujana *et al.* [50] was prepared nano-ceria by surfactant-mediated precipitation technique in mixed solvent system. The CeO_2 obtained from this method shows good thermal stability and the surface area of sample calcined at 400°C was found to be 133 m^2/g.

---

[*]Supakanapitak, S., Boonamnuayvitaya, V. and Jarudilokkul, S., 2012, "Synthesis of nanocrystalline CeO_2 particles by different emulsion methods", Materials Characterization, doi: 10.1016/j.matchar.2012.02.018

In this work, the experiment is divided into two parts. Firstly, the three different types of microemulsion (RM, ELM, and CEAs) were used for prepared CeO_2. Then, the suitable method of preparation which provided nanometer particle size, high surface area, and high purity was selected. Secondly, the effect of cerium source, surfactant type, calcination temperature, and the water content on the CeO_2 powders were investigated. X-ray diffraction (XRD), BET surface area analysis, dynamic light scattering (DLS) and transmission electron microscopy (TEM) were utilized to characterize prepared CeO_2 powder. Thermal analysis was performed by thermo-gravimetrically (TG-DTG) and differential scanning calorimetry (DSC).

4.2 Objectives

1) To synthesize the nano-sized CeO_2 particles by different microemulsion methods.

2) To investigate the effect of cerium source, surfactant type, calcination temperature, and the water content on the CeO_2 powders.

4.3 Working scopes

1) Determine the suitable microemulsion method (RM, ELM, and CEAs) that gives the smallest particle size and the highest yield, surface area, and purity.

2) At the most suitable preparation method, determine the most suitable conditions of synthesized CeO_2 powder (Cerium sources: $(NH_4)_2Ce(NO_3)_6$, $Ce(NO_3)_3 \cdot 6H_2O$, and $CeCl_3 \cdot 7H_2O$, surfactant type: PE4LE, Brij52, Brij96, AOT and CTAB, calcination temperature ranges between 500-900°C, and the water content ranges between 3-7 ml.

4.4 Experimental

4.4.1 Materials

Ammonium cerium nitrate ($(NH_4)_2Ce(NO_3)_6$) and Polyoxyethylene-4-luaryl ether (PE4LE) were chosen as the cerium source and surfactant for study of the preparation by different three microemulsion methods (reversed micelle (RM), emulsion liquid membrane (ELM), and colloidal emulsion aphrons (CEAs)). Hexane (C_6H_{14}) was used as organic solvent and hydrazinium hydrate ($N_2H_4 \cdot H_2O$) was used as reducing agent. The precipitate was washed with ethanol (C_2H_5OH). In CEAs method used

Polyoxyethylene sorbitan monooleate (Tween80) to form colloidal gas aphrons. For study the effect of the type of cerium source was used cerium nitrate hexahydrate ($Ce(NO_3)_3 \cdot 6H_2O$) and cerium chloride heptahydrate ($CeCl_3 \cdot 7H_2O$). The effect of surfactant type was used polyoxyethylene-10-oleyl ether (Brij96V), polyoxyethylene-2-cetyl ether (Brij52), sodium bis (2-ethyl hexyl) sulfosuccinate (AOT), and cetyltrimethylammonium bromide (CTAB). The chemical structures of all surfactants were shown in Figure 4.1.

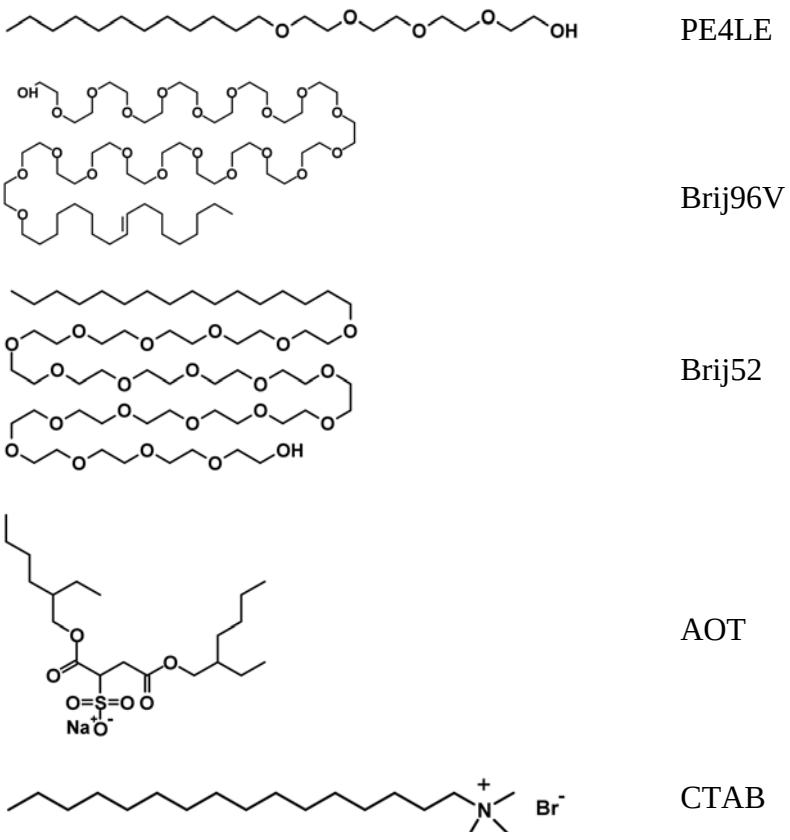

Figure 4.1 The chemical structure of all surfactants.

4.4.2 Preparation of nano-sized CeO_2 by different microemulsion methods

4.4.2.1 Reversed Micelle (RM)

In typical preparation of nano-sized CeO_2, $(NH_4)_2Ce(NO_3)_6$ (2.5 g) was dissolved in 0.1 ml of distilled water and then added into 70 ml of n-hexane. An appropriate amount of PE4LE was added to the solution under vigorous stirred until all $(NH_4)_2Ce(NO_3)_6$ completely dissolved in the solution and transparent micoemulsion was obtained. Then $N_2H_4 \cdot H_2O$ was added into the solution to neutralize the cerium ion in the reverse

micelles. The hydrazine in the amount of 5% of total volume is sufficient to ensure that reduction takes place without destroying the isotropic solution. The mixtures of the solution were centrifuged at 12,000 rpm for 15 min to separate the precipitate from solution. The brown precipitate was washed with ethanol and centrifuged for 2 times in order to completely remove both residual phase and organic phase. The precipitate was dried at 100°C for 1 h and finally was calcined at 500°C for 3 h. The schematic procedure is illustrated in Figure 4.2.

4.4.2.2 Emulsion Liquid Membrane (ELM)

An internal phase of W/O emulsion was $N_2H_4 \cdot H_2O$ solubilized in the organic membrane phase comprise n-hexane (70 ml) and PE4LE (12 ml). The mixed solution was stirred at 500 rpm for 30 min then the W/O emulsion was obtained. The W/O emulsion was added to an external water phase containing $(NH_4)_2Ce(NO_3)_6$ (2.5 g) and deionized water. Stirring at vigorously speed was required to disperse W/O emulsion droplet to form W/O/W emulsion. After stirring for 1 h, the mixed solution turned dark brown. Then, it was placed into a centrifuge tube for centrifugation at a speed of 12,000 rpm for 15 min to separate the precipitate from solution. The precipitate was washed with ethanol followed by centrifugation in order to completely remove both residual external phase and organic membrane phase for 2 times. The precipitate was dried at 100°C for 1 h and finally was calcined at 500°C for 3 h. The schematic procedure is illustrated in Figure 4.3.

4.4.2.3 Colloidal Emulsion Aphrons (CEAs)

The W/O emulsion (as described in the ELM preparation) was added to the colloidal gas aphrons (CGAs) by stirring vigorously. The colloidal gas aphrons were prepared by adding Tween80 (3 ml) into deionized water (30 ml) and mixing with a homogenizer at the rotation of 14,000 rpm for 2 min. After stirring for 1 h the colloidal emulsion aphrons (CEAs) were obtained. Then, an external water phase containing $(NH_4)_2Ce(NO_3)_6$ (2.5 g) and deionized water was added and stirred into the CEAs. The mixed solution was stirred at 500 rpm for 30 min. After stirring, the mixed solution turned dark brown which was then placed into centrifuge at a speed of 12,000 rpm for 15 min to separate the precipitate from the solution. The precipitate was washed with ethanol followed by centrifugation for 2 times in order to completely remove both residual external phase and organic membrane phase. The precipitate was dried at

100°C for 1 h and finally was calcined at 500°C for 3 h, and then CeO_2 powder was obtained. The schematic procedure is illustrated in Figure 4.4.

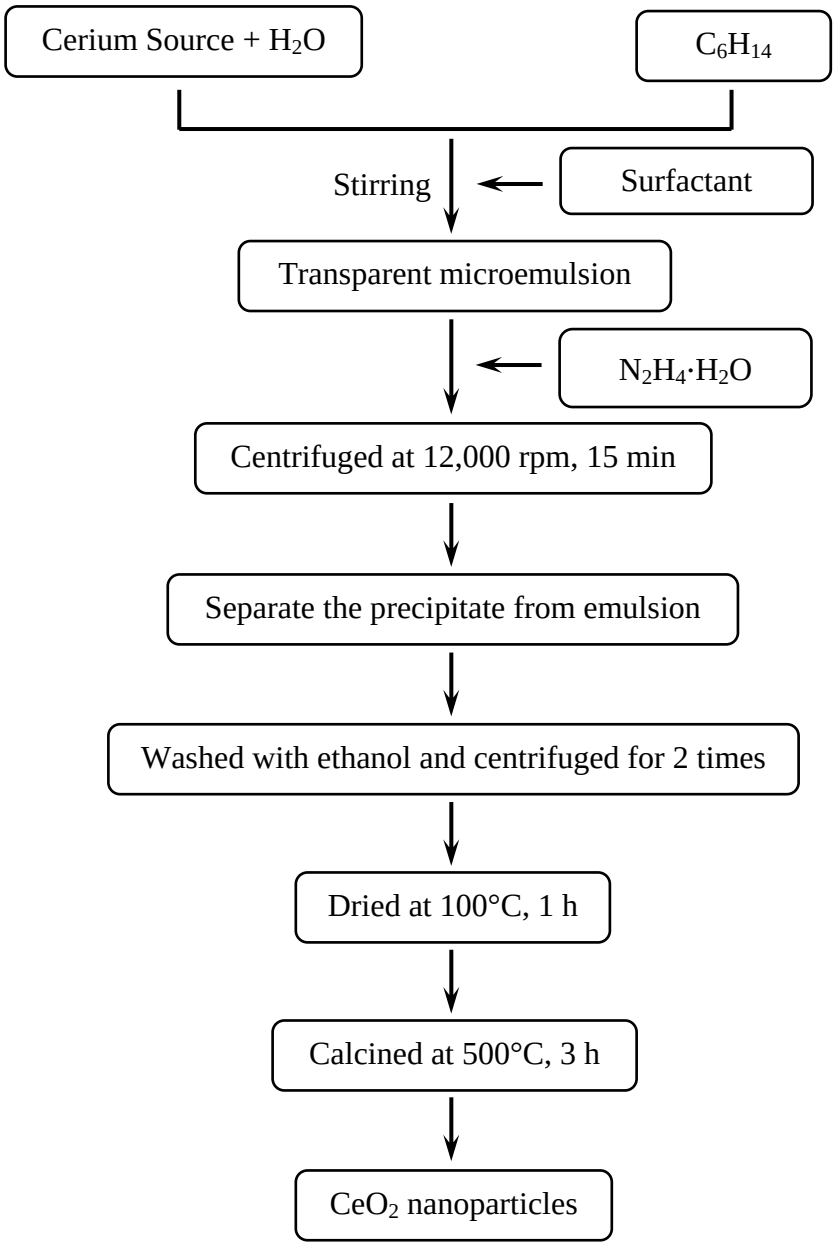

Figure 4.2 The schematic procedure of reversed micelle.

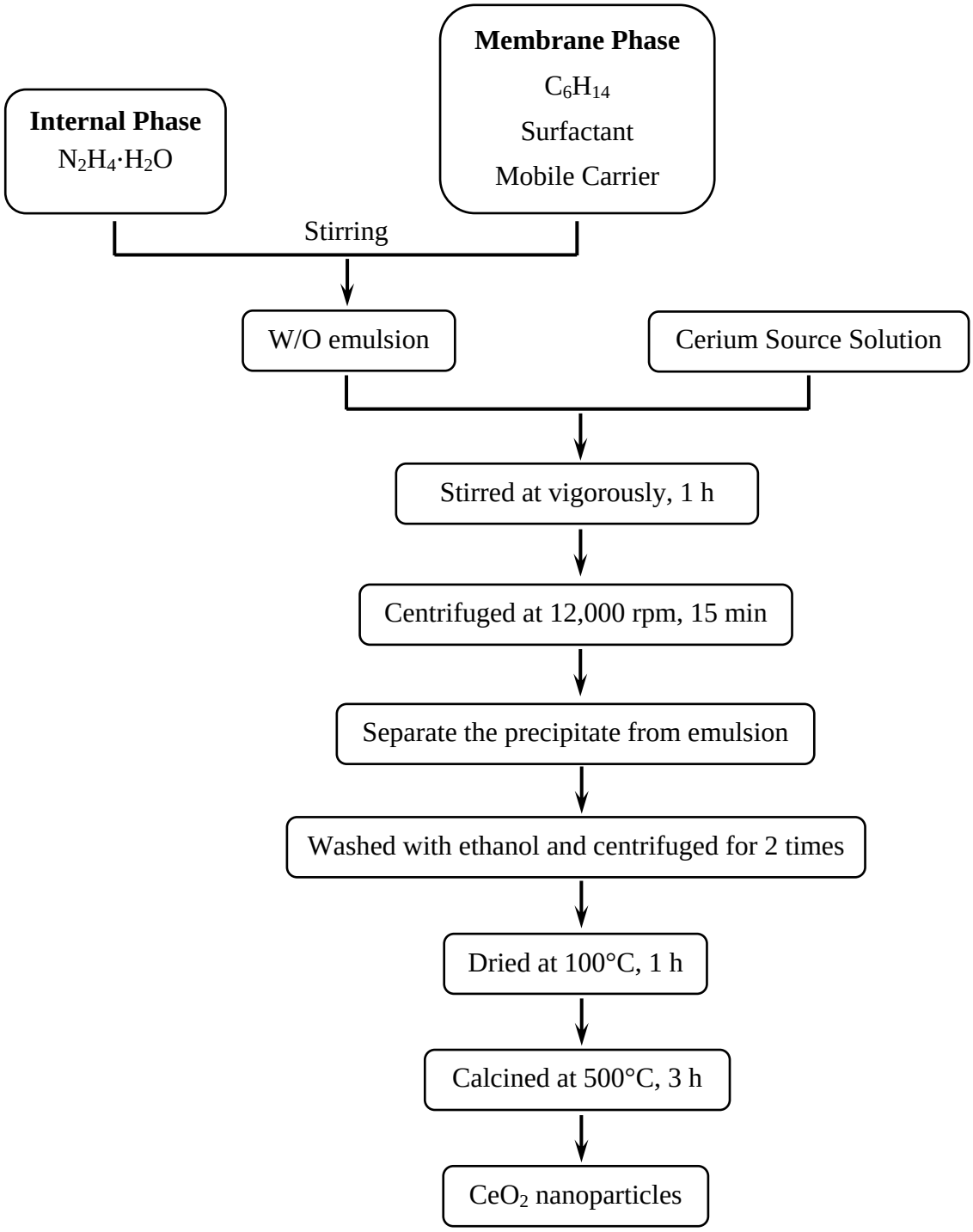

Figure 4.3 The schematic procedure of emulsion liquid membrane.

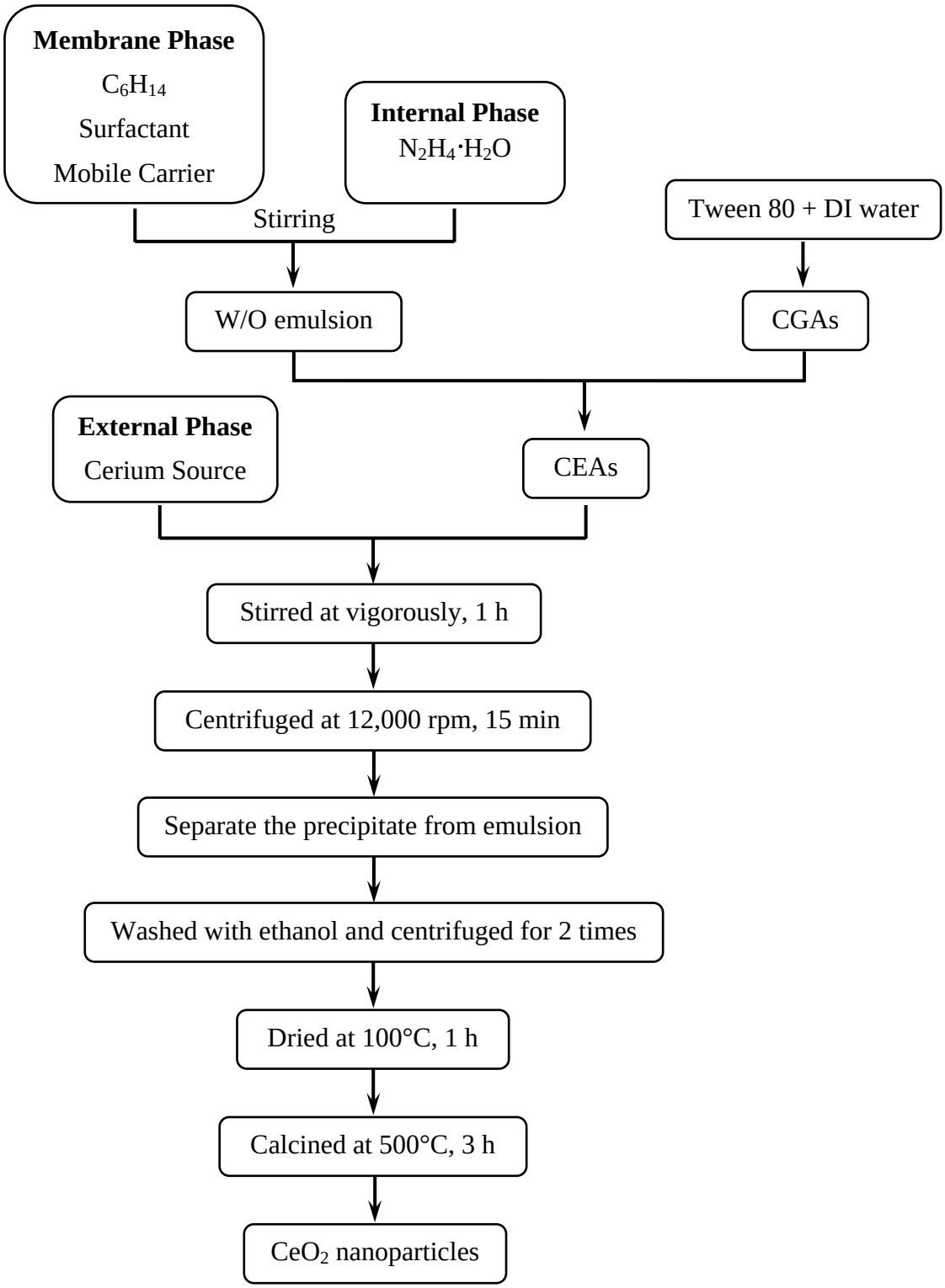

Figure 4.4 The schematic procedure of colloidal emulsion aphrons.

4.4.3 Characterization techniques

The objective of characterization is to examine the powder surface and bulk properties that may provide substantial information about the powder attributes. The information from various characterization tools will significantly improve the understanding of how the physicochemical attributes and powder performances are related. This section give a brief review of the basic concepts of various powder characterization techniques applied in this study, namely XRD, TEM, TGA-DTG, DSC, DLS, surface area, pore size analysis and nitrogen adsorption/desorption analysis. Each characterized method is discussed below.

4.4.3.1 X-ray Diffraction

X-ray diffraction (XRD) spectroscopy has been commonly used for crystalline phase's identification and the average crystallite size determination in a powder sample. The XRD pattern of material is like a fingerprint of the material. The powder diffraction method is ideally suitable for characterization and identification of a polycrystalline phase. When X-rays interact with a crystalline material, a diffraction pattern is achieved. Every crystalline material gives a pattern; the same material always gives the same pattern. Our aim is to see diffraction pattern is a pure CeO_2 for each preparation method and how the diffraction changed with the factors that studied.

The powder is irradiated with an X-ray of known wavelength, and hence diffraction of the X-ray takes place. The angle at which constructive interference occurs is then measured and the interplanar spacing (d spacing) of the crystals can be evaluated using Bragg's Law [51], as shown in equation (4.1):

$$n\lambda = 2\,d\sin\theta \tag{4.1}$$

where n is the order of diffraction (integer), λ is the incident X-ray wavelength (Å), d is the spacing between atomic layers in crystal (Å), and θ is the angle between the incidence ray and the scattering plane (degree)

The XRD patterns of the CeO_2 were carried out in a Bruker D8 Discover diffractometer using CuKα radiation (λ = 1.542 Å) operating at 40 kV and 40 mA, scaned rate at 0.02 degree/step over the angular ranges of 2θ = 20-100°. The crystallite size of sample

powder (d_{XRD}) was estimated by applying full-width-half-maximum (FWHM) of characteristic peak (111) to the Scherrer equation (equation (4.2)) [2]:

$$d_{XRD} = k\lambda/\beta cos\theta \quad (4.2)$$

Where λ is the wavelength of the X-ray used (Å), β is the half height width of the characteristic peak, θ is the diffraction angle for the (111) plane and k is Scherrer's constant ranging from 0.7 to 1.71. The value of k is used as 0.9 in this study.

4.4.3.2 Thermogravimetric Analysis

The thermal analysis was carried out in order to evaluate the chemical composition of the CeO_2 and elucidate the transformation of crystalline CeO_2. The thermal analysis were performed by thermogravimetry carried out on a Shimadzu TA-50 thermal analyzer at the heating rate of 10°C/min from room temperature to 1000°C in air atmosphere. Differential scanning calorimetry (DSC) carried out on a Star^{e}system METTLER TOLEDO at a heating rate of 10°C/min from room temperature to 550°C. Our aim of the thermal analysis is to confirm the purity of synthesized powders of CeO_2.

4.4.3.3 Transmission Electron Microscope

Transmission electron microscope (TEM) is an imaging technique whereby a beam of electrons is transmitted through a specimen, then an image is formed, magnified and directed to appear either on a fluorescent screen or layer of photographic film or to be detected by a sensor such as a CCD camera. TEM investigations were performed on Jeol Model JEM-2100 with 100 kV of accelerating voltage. The samples were prepared by allowing an ethanol suspension of the finely ground powder to evaporate on a copper grid coated with a holey carbon film. The average particle size of synthesized powder from TEM images were measured by IQ Materials Program.

4.4.3.4 Specific surface area, pore volume and nitrogen adsorption/desorption analysis

Since most powders are porous in nature with deep and complex network of pores, the determination of specific surface area is generally considered an important powder characterization. Beside the liquid-solid interface adsorption and the mercury

porosimetry, the gas adsorption methods are the most widely used to determine the surface area and pore size distribution. Analysis involves adsorption of nitrogen gas onto the surface and into the pores of outgassed sample. A know amount of nitrogen gas is added into an evacuated tube containing the sample. The quantity of adsorbed gas and the pressure in the sample tube is incrementally increased with a constant tube temperature. After each dose of nitrogen gas, when the pressure in the sample is equilibrated, the data is recorded. Pressure readings are used to calculate the gas volume adsorbed. The volume of gas adsorbed is measured as a function of relative pressure. Relative pressure is defined as the ratio of pressure in the sample tube to the saturation vapor pressure of adsorbed gas. The sample tube is immersed in a Dewar (vacuum flask) filled with liquid nitrogen to maintain a temperature where liquefaction of nitrogen gas can take place on the sample. The resulting data set is called an adsorption isotherm which is used to calculate the surface area.

The nitrogen adsorption/desorption isotherm was obtained at liquid nitrogen temperature 77 K by using Quantachrome. Autosorb-l surface area and pore size analyzer. Prior to measurement, all synthesized powder was outgas at 250°C under nitrogen flow for 5 h. The total surface area was determined using multi-point BET method by an Autosorb-l from Quantachrome Instruments, together with the determination of the pore volume as well as the pore size distribution of the sample. Our aim of the nitrogen adsorption/desorption analysis is to assess how the specific surface area, pore volume, and pore size of the synthesized powders varied with the preparing conditions.

4.4.3.5 Dynamic light scattering technique

Dynamic light scattering technique (DLS) has been commonly used for measured the size and zeta-potential to optimize stability and shelf life and speed up formulation development. The emulsion systems were characterized by dynamic light scattering using a Zetasizer nano ZS from Malvern Instrument. The emulsion droplet size evaluated by DLS measurement use the n-hexane viscosity for calculation the droplet size by Stoke-Einsten equation. Our aim of dynamic light scattering is to measure the size of emulsion droplet prepared by different methods.

4.5 Results and discussion

4.5.1 Characterization of CeO_2 prepared by different microemulsion methods

Figure 4.5 shows the XRD patterns of the synthesized powders obtained from different methods of preparation. All the reflection in Figure 4.5 can be indexed to pure crystalline CeO_2. The characteristic peaks corresponding to (111), (200), (220) and (300) planes are located at 2θ = 28.78°, 33.13°, 48.12° and 56.81°, respectively and no impurity peaks are observed in the patterns. The peaks are close to the ones of the face centered cubic fluorite structure of CeO_2 with lattice parameter is 5.4113Å (standard data JCPDS 34-0394). The crystallite size was calculated by the Scherrer equation from the (111) XRD peak as shown in Table 4.1. The crystallite size of CeO_2 obtained from CEAs is the smallest; the width of the peaks was broad because of their fine particle size. However, the peak obtained from CEAs was broadened than that of ELM and RM. The result was agreed with the crystallite size of CeO_2 obtained from CEAs the smallest.

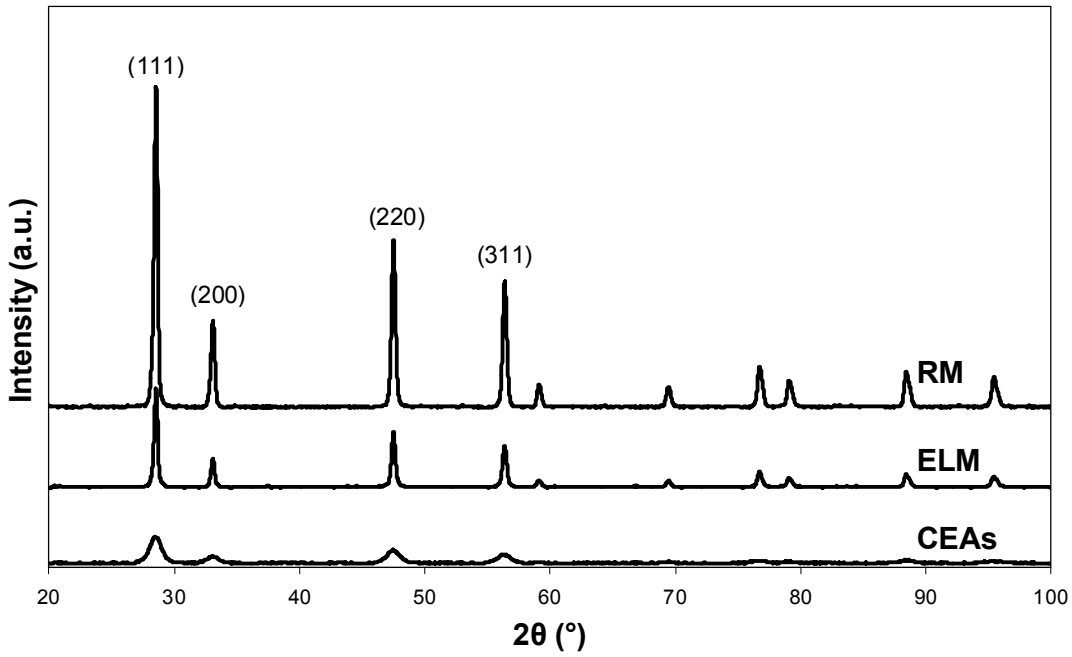

Figure 4.5 XRD patterns of CeO_2 prepared by (a) RM, (b) ELM, and (c) CEAs.

Figure 4.6 shows the TEM micrographs of CeO_2 obtained from preparation by different methods. It is evident from the figure that the particles were small, have a similar

morphology and exhibit a very narrow particles size distribution. The average particle size of CeO_2 prepared by RM, ELM and CEAs were 9.4 ± 0.2, 5.8 ± 0.2 and 4.7 ± 0.1 nm, respectively. However, this result shows that the average particles size of CeO_2 prepared by CEAs (in Figure 4.6 (c)) was the smallest. There is a slight difference between the average particle size from TEM micrograph and crystallite size from XRD peak, which belongs to range of the standard deviation. This agreed relatively well with the calculated values by XRD analysis.

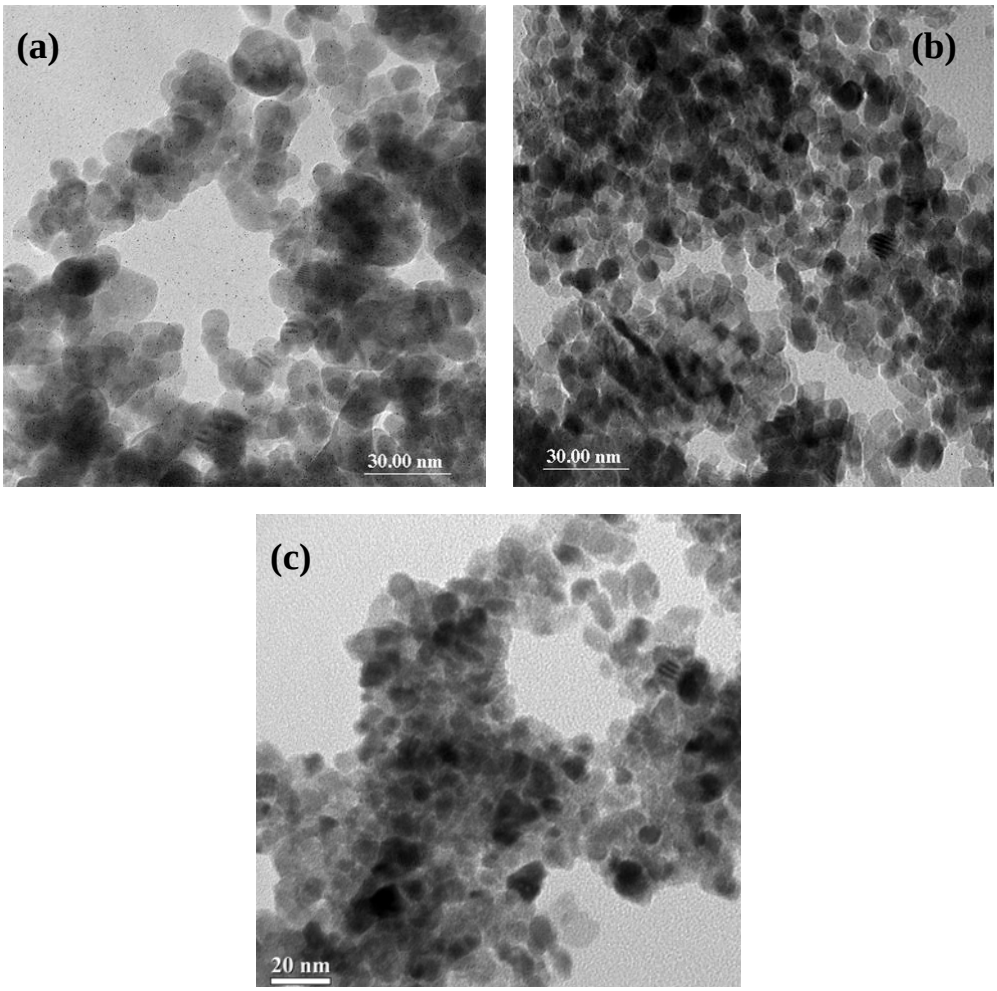

Figure 4.6 TEM micrographs of CeO_2 prepared by (a) RM, (b) ELM, and (c) CEAs.

When considering the average particle size of CeO_2 obtained from different methods with the same starting material, it was found that the average particles size of CeO_2 prepared by CEAs is the smallest. The particles size prepared by the emulsion method can be controlled by the micro-droplet size of the inner phase. In colloidal emulsion aphrons (CEAs), the inner phase within the emulsion core is encapsulated by a soapy

shell consisting of multi-layer of surfactant molecules [23]. Therefore, when the stable nucleus of cerium was formed, it enlarged through the growth and aggregation of primary particles. As the particles reached the water droplets in inner phase the surfactant would cover the particles' surface and hinder further particles from growing, which also restricted the size of particles. Therefore, the emulsion droplet size prepared from the different methods was examined by dynamic light scattering (DLS) particle size distribution analysis, as shown in Figure 4.7. It was found that the emulsion droplet of CEAs was the smallest size, and this result agreed with the result from TEM.

The surface area and porosity analysis are presented in Table 4.1. The result showed that the surface area of CeO_2 prepared by CEAs was tenfold higher than other methods and showed higher percent yield. The porosity analysis results showed that CeO_2 prepared by CEAs method has the highest pore volume and the smallest pore size. Therefore, the surface properties of CeO_2 particles prepared by CEAs have many small pores, while the CeO_2 particles prepared by RM and ELM have less big pores, resulting in the highest surface area. Figure 4.8 displays the isotherms of prepared CeO_2 by different methods. The isotherms were similar to type IV isotherm with a hysteresis loop for all CeO_2. The hysteresis loops of CeO_2 prepared by RM and ELM were similar to type H3 shape corresponding to the adsorption in slit-shaped pored, while the hysteresis loops of CeO_2 prepared by CEAs similar to type H1 shape corresponding to the adsorption in regular pored and narrow size distribution and type H1 are often obtained with agglomerates of compacts of spheroidal particles of fairly uniform size and array [39].

Table 4.1 Surface area, porosity, average particle size, and percent yield of CeO_2 prepared by different methods.

Method	Surface area (m^2/g)	Pore volume (cm^3/g)	Pore size (Å)	Crystallite size (nm)	Average particle size (nm)	%Yield
RM	5.32	0.0548	411.8	9.56	9.4 ± 0.2	32.75
ELM	9.77	0.0673	275.5	5.93	5.8 ± 0.2	48.75
CEAs	145.73	0.2170	59.5	4.79	4.7 ± 0.1	84.29

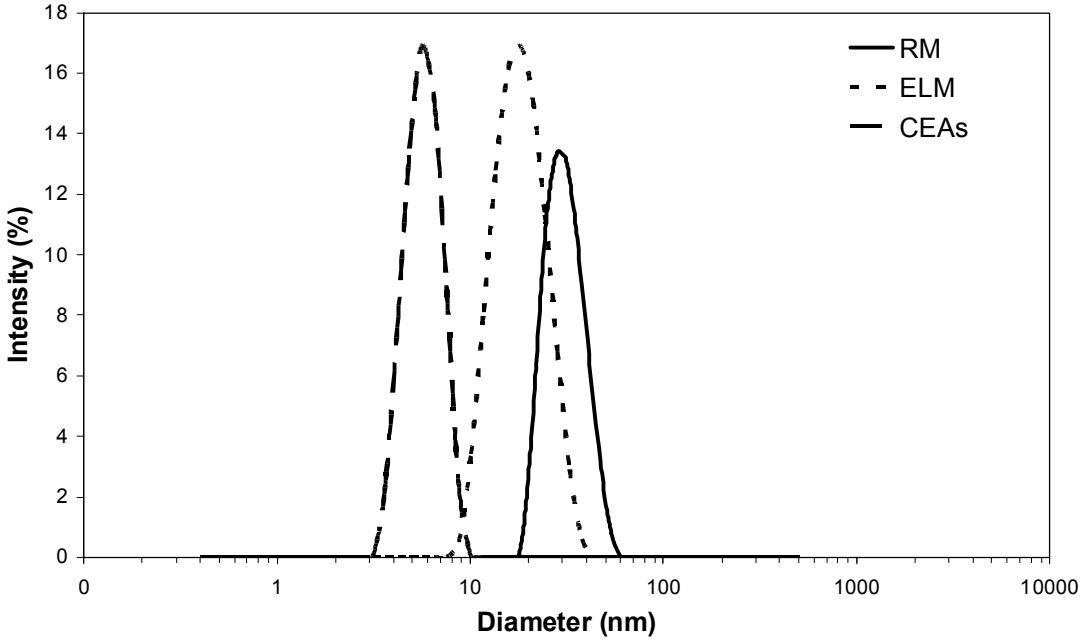

Figure 4.7 The emulsion droplet size distribution prepared by different methods.

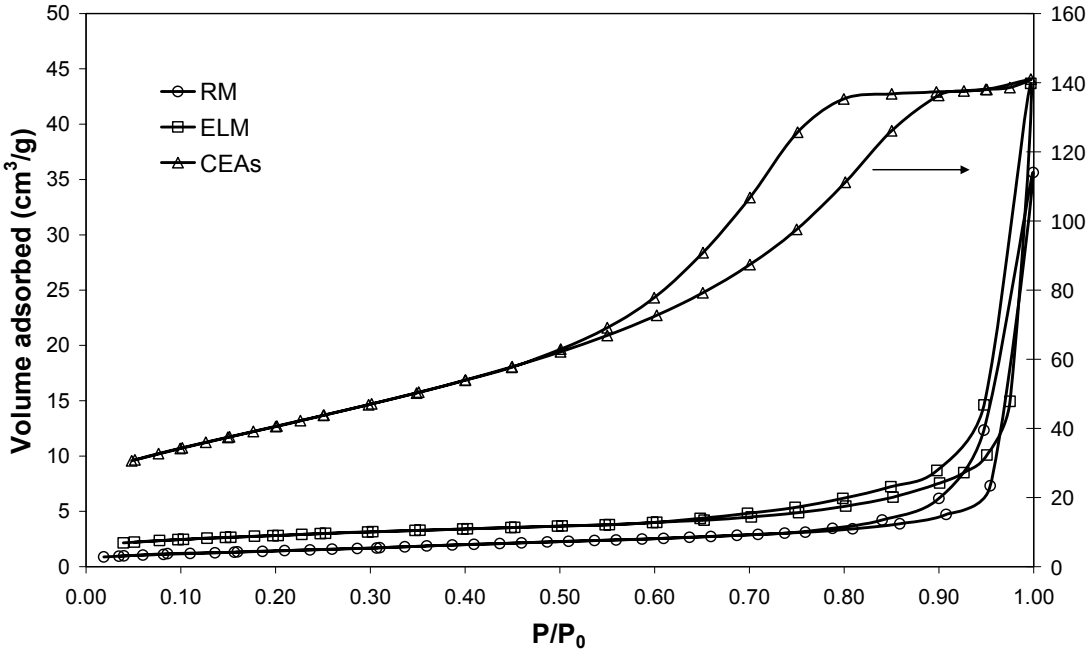

Figure 4.8 Adsorption-desorption isotherms of CeO_2 prepared by different methods.

The results from TEM, BET, and DLS indicated that CeO_2 prepared by CEAs method showed the smallest particle size, the highest surface area, and the smallest emulsion droplet which meant this method was suitable to prepared nano-sized particles.

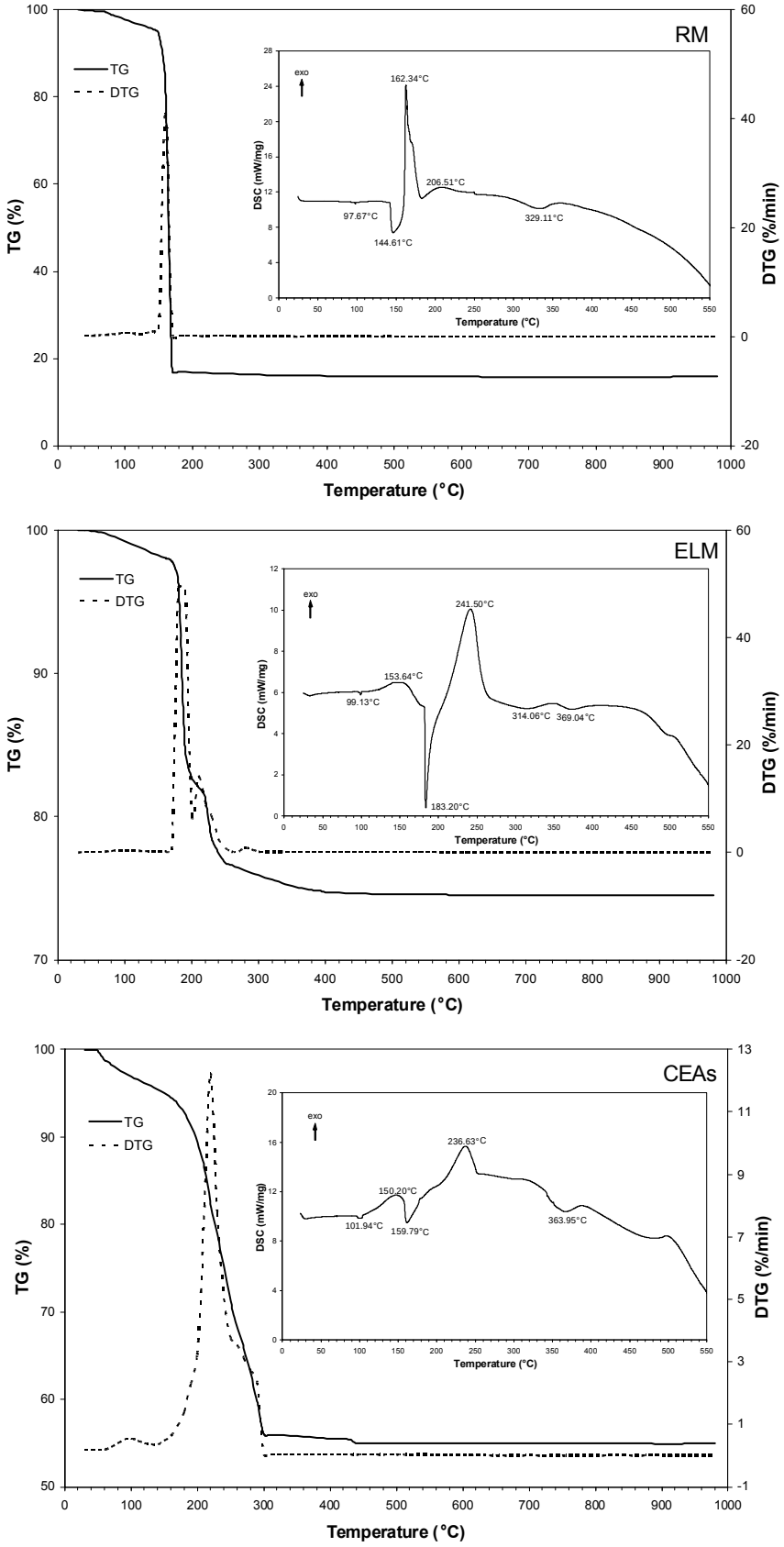

Figure 4.9 Thermal analysis of synthesized powders prepared by different methods.

The thermal analysis was carried out in order to evaluate the chemical composition of the CeO_2 and elucidate the transformation of crystalline CeO_2. The thermal analysis of CeO_2 prepared by different emulsion methods are given in Figure 4.9. Three major weight losses are seen in all preparation. The first step (I) observed at around 70-150°C is associated with a weight loss of 5.21% for RM and 70-180°C showed a weight loss of 3.55% and 5.50% for ELM and CEAs, respectively. The weight losses was lower than those corresponding to the decomposition of $Ce(OH)_3$ (9.95%) or $Ce(OH)_4/CeO_2{\cdot}2H_2O$ (17.3%) [34]. It is well known that the weak DSC peak around 100°C for all preparation, associating with the low weight loss on the TG curve, which are related to the dehydration of adsorbed water from the sample. The second (II) weight loss appeared at 150-170°C, 180-250°C and 180-300°C with a mass loss of 77.6%, 19.67% and 37.81% for RM, ELM and CEAs, respectively. It can be found that there are obvious endothermic peak around 145°C, 183°C and 160°C for RM, ELM and CEAs, respectively, associating with the sharp weight loss on the TG curve, indicated to the decomposition of hydrated oxide to CeO_2. The poorly resolved third (III) step accounted for 1.02%, 2.09% and 1.06% weight losses for RM, ELM and CEAs, respectively, which represented decomposition of surfactant and other organic compounds. The total weight loss of CeO_2 prepared by the RM, ELM and CEAs were 84.08, 26.06 and 44.97%, respectively. The thermal analysis results showed that there were no weight losses at temperatures higher than 450°C indicating the crystalline CeO_2 formation as the final product. Therefore, the CeO_2 samples obtained from the three methods and calcined at 500°C are purity confirmed by thermal analysis.

4.5.2 Influence of various factors on the average particles size and surface area

The results from XRD, DLS, TEM and BET indicated that all the synthesized powders were cubic fluorite structure CeO_2 nanoparticles. The preparation of CeO_2 by the colloidal emulsion aphrons shows the highest surface area and the smallest in particle size. Therefore, the suitable conditions of synthesized CeO_2 were studied.

4.5.2.1 The type of cerium source

Figure 4.10 shows the XRD patterns of the products prepared by the CEAs method using different cerium sources. All the reflection in figure can be indexed to pure crystalline CeO_2 and no impurity peaks were observed in the patterns. The peaks are

close to the ones of the face-centered cubic fluorite structure of CeO_2 with lattice parameter is 5.4113 Å (standard data JCPDS 34-0394).

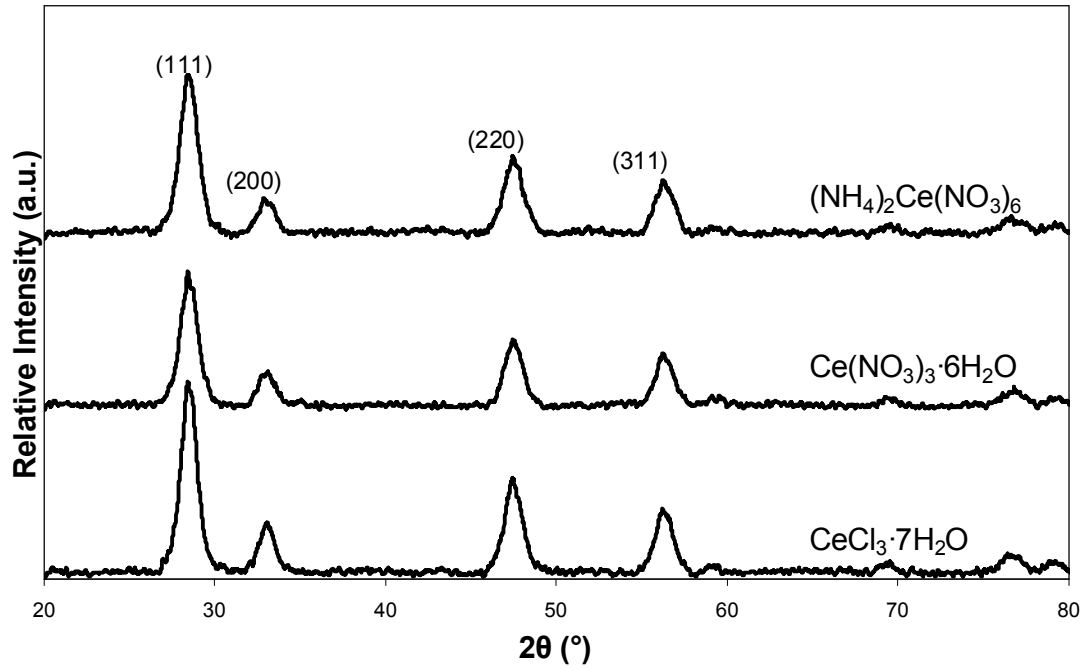

Figure 4.10 XRD patterns of CeO_2 prepared by CEAs using different cerium sources.

Figure 4.11 shows the TEM micrographs of CeO_2 prepared by the CEAs method using different cerium sources. It is evident from the figure that the particles were small in size and uniform in shape. The average particle size of CeO_2 obtained from $(NH_4)_2Ce(NO_3)_6$, $Ce(NO_3)_3{\cdot}6H_2O$ and $CeCl_3{\cdot}7H_2O$ as a cerium source were 4.7 ± 0.1, 5.4 ± 0.2 and 5.9 ± 0.2 nm, respectively, and the particle sizes are distributed in a very narrow range. The surface tensions of all cerium sources are listed in Table 4.2. It was found that the average size of CeO_2 particles changed slightly with the change of cerium sources. The average particle size slightly increases with the increasing of surface tension. As a cerium compound that has low surface tension can disperse to smaller droplets in emulsion easily resulting in small particles should be produced. Therefore, the influence of the cerium source is slightly apparent. The surface areas of CeO_2 prepared by $(NH_4)_2Ce(NO_3)_6$, $Ce(NO_3)_3{\cdot}6H_2O$ and $CeCl_3{\cdot}7H_2O$ were 145.73, 142.23 and 141.56 m^2/g, respectively. The result shows that the surface areas were nearly the same, On the other hand, the surface area obtained from $(NH_4)_2Ce(NO_3)_6$ is higher than the others.

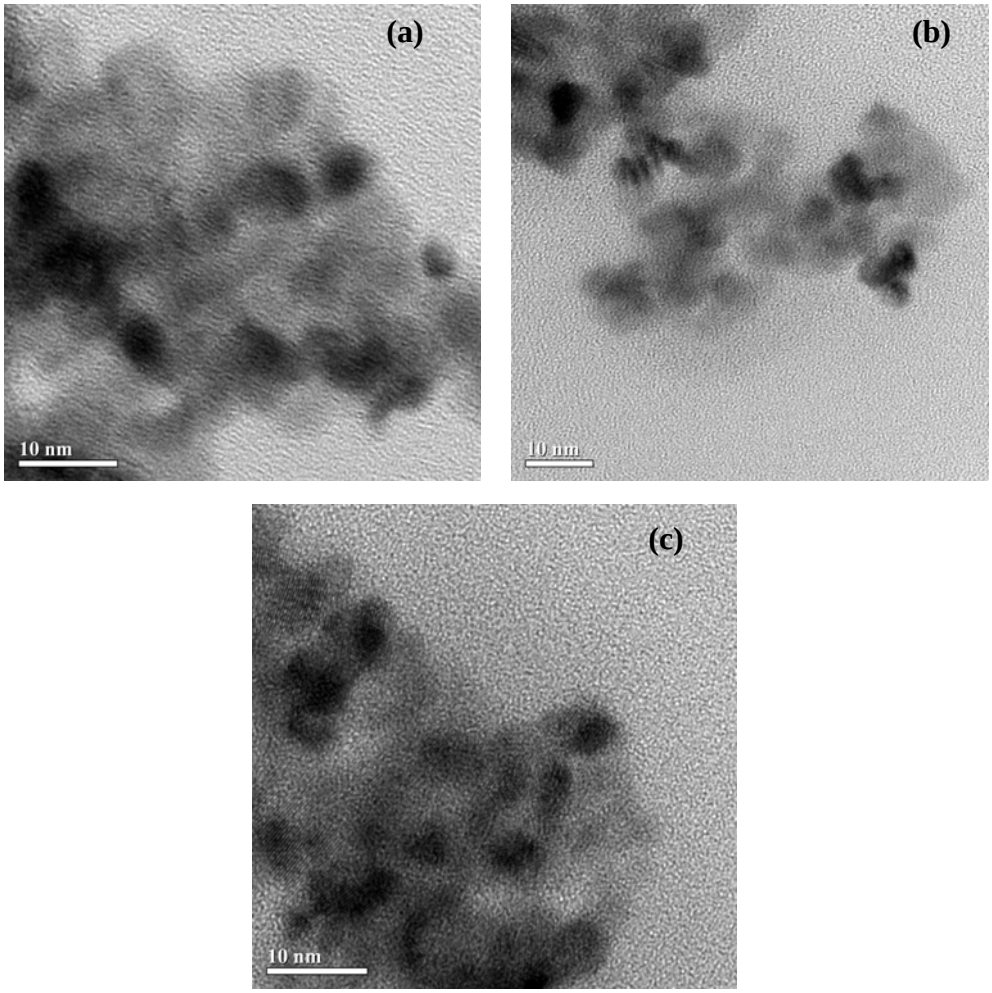

Figure 4.11 TEM micrographs of CeO_2 prepared by CEAs method using different cerium sources (a) $NH_4)_2Ce(NO_3)_6$, (b) $Ce(NO_3)_3 \cdot 6H_2O$, and (c) $CeCl_3 \cdot 7H_2O$.

Table 4.2 Surface tension of aqueous cerium compound and the average particle size of CeO_2 prepared by different cerium sources.

Cerium source	**Surface Tension (mN/m)**	**Average particle size (nm)**
$(NH_4)_2Ce(NO_3)_6$	63.23	4.7 ± 0.1
$Ce(NO_3)_3 \cdot 6H_2O$	64.92	5.4 ± 0.2
$CeCl_3 \cdot 7H_2O$	65.35	5.9 ± 0.2

The surface area of CeO_2 prepared by CEAs method used $(NH_4)_2Ce(NO_3)_6$, $Ce(NO_3)_3 \cdot 6H_2O$ and $CeCl_3 \cdot 7H_2O$ as cerium source were 145.7, 138.8 and 139.5 m^2/g, respectively. The result shows that the surface area nearly the same. On the other hand, surface area obtained from $(NH_4)_2Ce(NO_3)_6$ was higher than the others and shows higher percent yield. The porosity analysis were summarize in Table 4.3.

Table 4.3 Surface area, porosity, average particle size and percent yield of CeO_2 prepared by different cerium sources.

Cerium source	Surface area (m^2/g)	Pore volume (cm^3/g)	Pore size (Å)	Average particle size (nm)	%Yield
$(NH_4)_3Ce(NO_3)_6$	145.7	0.217	59.5	4.7 ± 0.1	84.29
$Ce(NO_3)_3 \cdot 6H_2O$	138.8	0.244	69.8	5.4 ± 0.2	81.21
$CeCl_3 \cdot 7H_2O$	139.5	0.204	58.3	5.9 ± 0.5	69.97

4.5.2.2 The type of surfactant

Figure 4.12 shows the XRD patterns of the products prepared by the CEAs method using different surfactants. All the reflection in Figure 4.12 could be indexed to pure crystalline CeO_2 and no impurity peaks were observed in the patterns. The peaks are close to the ones of the face-centered cubic fluorite structure of CeO_2 with lattice parameter is 5.4113 Å (standard data JCPDS 34-0394).

Figure 4.13 shows the TEM micrographs of CeO_2 prepared by the CEAs method using different surfactant. It is evident from the figure that the particles were small in size and uniform in shape. The average particle size of CeO_2 obtained from PE4LE, Brij96V, Brij52, AOT and CTAB were 4.7 ± 0.1, 4.5 ± 0.2, 4.6 ± 0.1, 4.1 ± 0.2 and 5.1 ± 0.1 nm, respectively. However, this result shows that the average particles size of CeO_2 obtained from AOT (in Figure 4.13 (d)) was the smallest. As expected, the size of CeO_2 particles prepared by all surfactants is distributed in a very narrow range.

The effect of the hydrophobic group of surfactant on the CeO_2 particle size was investigated in the CEAs method using nonionic surfactants. When considering the average size of CeO_2 particles with different nonionic surfactants it was found that the

average size obtained from Brij96V was the smallest. The average size obtained from Brij52 was smaller than that from PE4LE. The studied surfactants are nonionic surfactant but Brij96V has the longest hydrocarbon chain (HC) length. If the hydrophobic hydrocarbon chain length is longer, the solubility of the surfactant in water decreases and its solubility in n-hexane increases [52], and surfactant tend to form aggregates which are call micelles. Since there are more micelles formed and the amount of water is the same, the size of water droplets in micelles are smaller resulting in smaller sizes of the particles. However, Brij96V shows the smallest average particle size but it difficult to form emulsion and used amount more than PE4LE to form emulsion at the same condition.

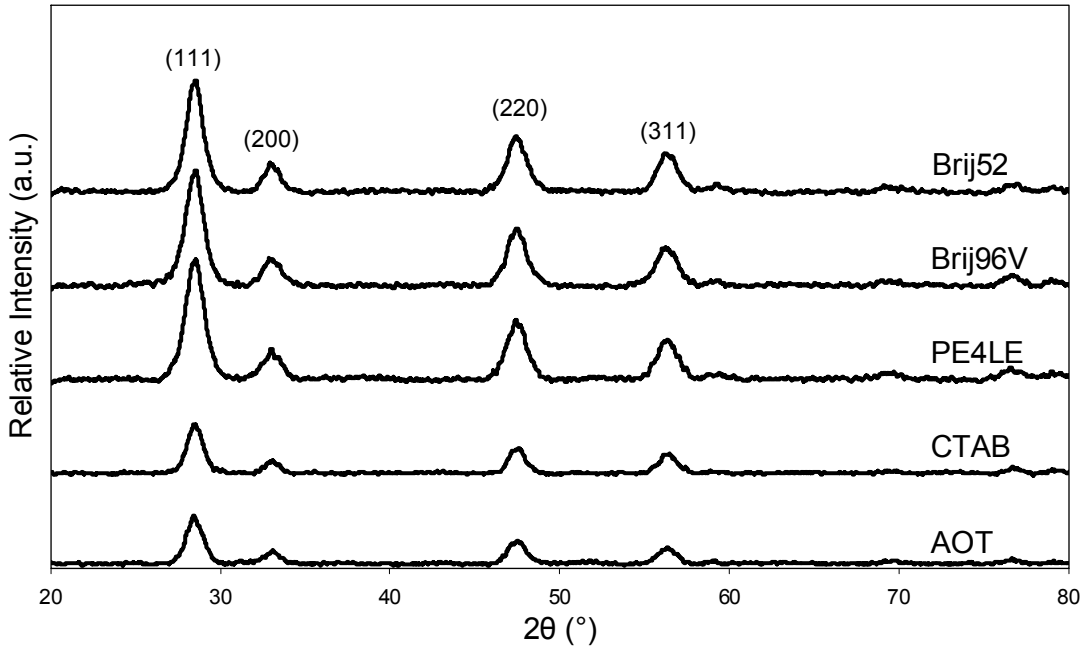

Figure 4.12 XRD patterns of CeO_2 prepared by CEAs using different surfactants.

The average particle size of CeO_2 prepared by using PE4LE and CTAB were 4.7 ± 0.1 and 5.1 ± 0.1 nm, respectively, while the particles prepared using AOT were as small as 4.1 ± 0.2 nm. It was considered that as the cerium ion has positive charge, AOT showed strong adsorption on the surface but CTAB might not be adsorbed on the surface. A certain repellent action exists between the hydrophilic group of CTAB and cerium cation at grain surface, which makes the stabilizing effect of CTAB on grain become weaker [33]. When nonionic surfactant (PE4LE) was used, the average particle size of CeO_2 was bigger than anionic surfactant. This result can be attributed to the stabilizing

effect of nonionic surfactant on water droplets and particles mainly derived from its hydrogen bond with water [6]. This action is weaker than that of ion bond.

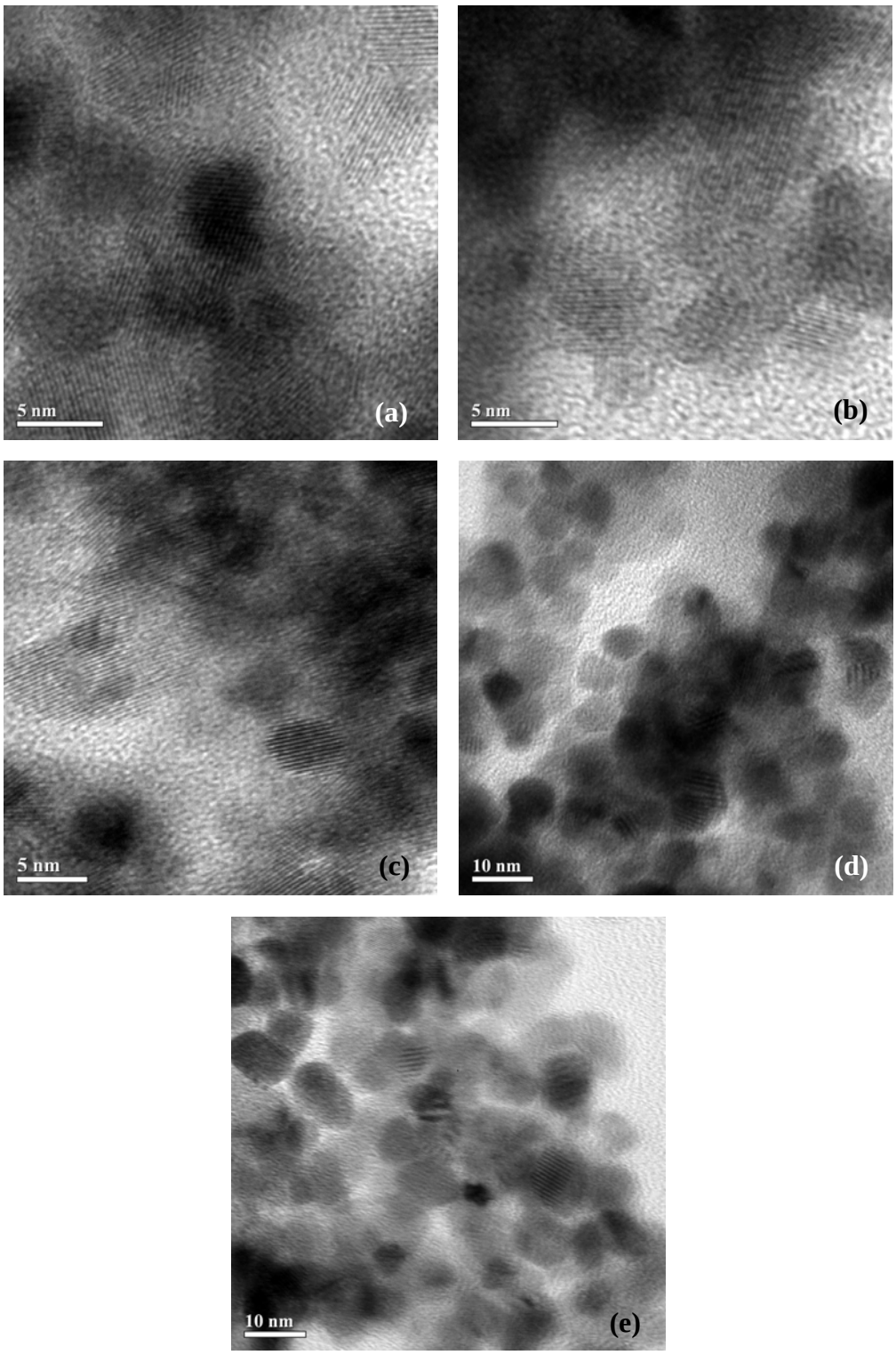

Figure 4.13 TEM micrographs of CeO_2 prepared by CEAs method using different surfactants (a) PE4LE, (b) Brij96V, (c) Brij52, (d) AOT, and (e) CTAB.

The surface area of CeO_2 prepared by PE4LE, Brij96V, Brij52, AOT, and CTAB were presented in Table 4.4. The result shows that the surface area obtained from Brij96V were the highest.

Table 4.4 Surface area, porosity, average particle size and percent yield of CeO_2 prepared by different surfactants.

Surfactant	Surface area (m^2/g)	Pore volume (cm^3/g)	Pore size (Å)	Average particle size (nm)	%Yield
PE4LE	145.7	0.217	59.55	4.7 ± 0.1	84.29
Brij96V	154.8	0.345	89.15	4.5 ± 0.2	78.30
Brij52	148.4	0.215	57.99	4.6 ± 0.1	78.38
AOT	102.5	0.171	66.65	4.1 ± 0.2	84.06
CTAB	34.6	0.115	132.70	5.1 ± 0.1	95.33

4.5.3.3 The calcination temperature

Figure 4.14 shows the XRD patterns of the products prepared by CEAs method carried out at different calcinations temperature. All the reflection in Figure 4.14 could be indexed to pure crystalline CeO_2 and no impurity peaks were observed in the patterns. The peaks are close to the ones of the face centered cubic fluorite structure of CeO_2 with lattice parameter is 5.4113 Å (standard data JCPDS 34-0394).

Table 4.5 summarizes the results of specific surface area, pore volume and average pore diameter of CeO_2 at different calcinations temperature. It was observed that after drying, specific surface area (S_{BET}) of CeO_2 was 201.40 m^2/g and surface area decreased at high calcination temperature. The results of total pore volume (V_T) showed similar trend as of S_{BET}. The decrease of micropore surface area (S_{mi}) with increasing of calcination temperature was also observed. It may be ascribed to the sintering impact.

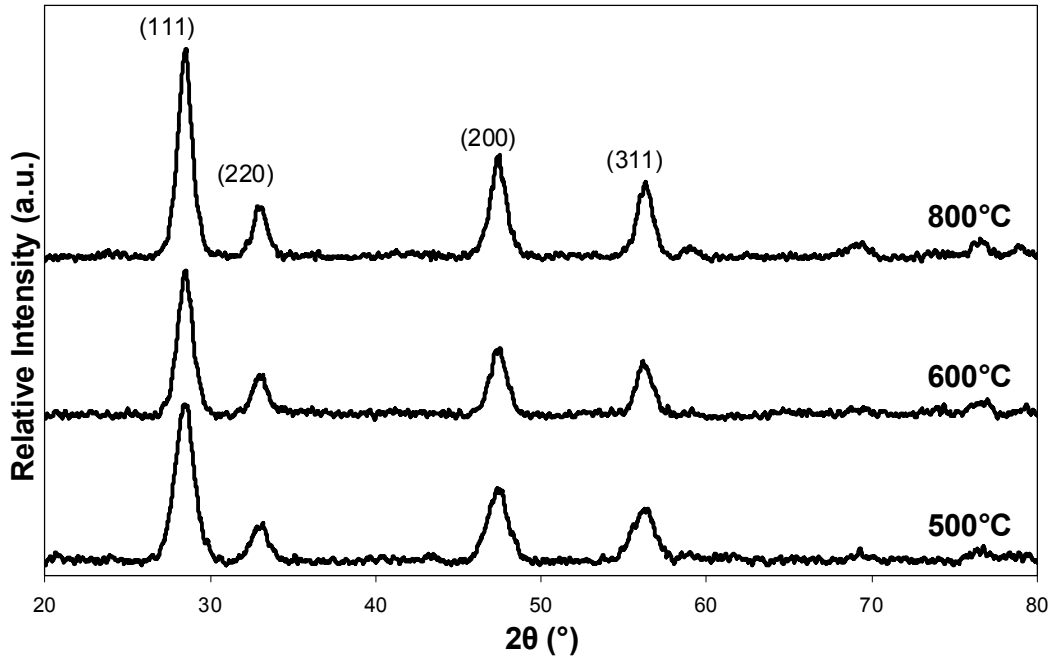

Figure 4.14 XRD patterns of CeO_2 prepared by CEAs method at different calcinations temperature.

Table 4.5 Total pore volume, surface area and average pore diameter of CeO_2 prepared by different calcinations temperature.

Catalyst	Pore volume (cm^3/g)			Surface area (m^2/g)			D
	V_T	V_{me}	V_{mi}	S_{BET}	S_{me}	S_{mi}	(Å)
CeO_2 (100°C)	0.1273	0.0278	0.0995	201.4	25.9	175.5	25.3
CeO_2 (200°C)	0.1781	0.1427	0.0354	175.3	164.0	11.3	38.7
CeO_2 (300°C)	0.1248	0.1006	0.0242	159.6	154.5	5.1	31.3
CeO_2 (400°C)	0.2155	0.2126	0.0029	155.7	147.8	7.9	55.4
CeO_2 (500°C)	0.2170	0.2158	0.0012	145.7	145.4	0.3	58.5
CeO_2 (600°C)	0.1747	0.1687	0.0060	137.7	137.5	0.2	69.8
CeO_2 (900°C)	0.0470	0.0470	0.0000	47.6	47.6	0.0	114.9

V_T: Total pore volume, V_{me}: Mesopore volume, V_{mi}: Micropore volume,

S_{BET}: BET surface area, S_{me}: Mesopore surface area, S_{mi}: Micropore surface area,

D: Average pore diameter.

Figure 4.15 shows the TEM micrographs of CeO_2 prepared by CEAs method carried out at different calcinations temperature in the range of 500-800°C. The average particle size of CeO_2 obtained from the calcination temperature of 500, 600, and 800°C were 4.7 ± 0.1, 7.6 ± 0.2, and 14.9 ± 0.2 nm, respectively. The average particle size of CeO_2 increased sharply with the rise of calcinations temperature. The observation could be explained as with the increase of calcination temperature, the growth rate of particles increases more rapidly than the nucleation rate does, and the aggregation trend of particles becomes stronger [6].

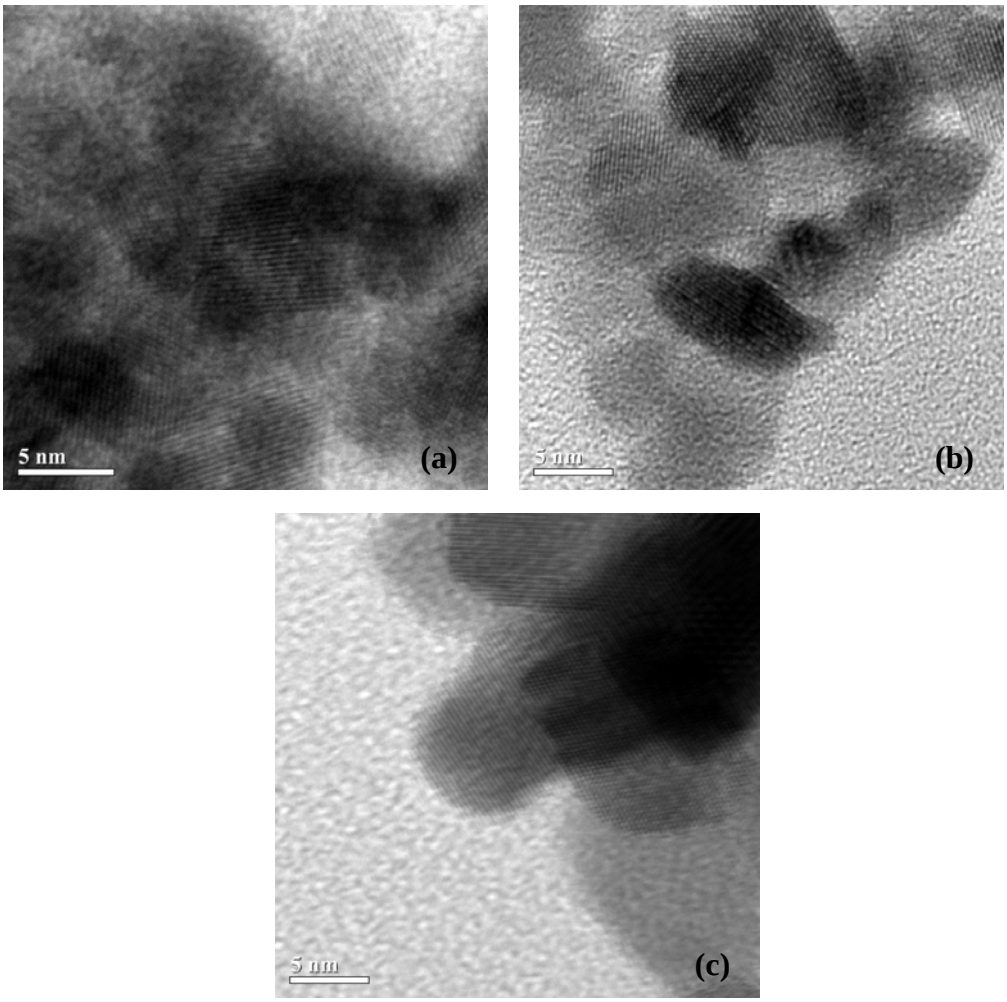

Figure 4.15 TEM micrograph of CeO_2 prepared by CEAs method at different calcinations temperature (a) 500°C, (b) 600°C and (c) 800°C.

4.5.3.4 The water content

Figure 4.16 shows the XRD patterns of the products prepared by CEAs method carried out at different calcinations temperature. All the reflection in Figure 4.16 could be indexed to pure crystalline CeO_2 and no impurity peaks was observed in the patterns. The peaks were close to the ones of the face centered cubic fluorite structure of CeO_2 with lattice parameter is 5.4113 Å (standard data JCPDS 34-0394).

The effects of water content are shown in Table 4.6. From table it was found that the crystallite size of CeO_2 was affected by water content. At water content of 3, 5 and 7 ml, the crystallite size were 5.81, 5.91 and 6.45 nm, respectively (calculated by equation (4.2)). The increase of water at constant concentration of surfactant caused the increase of crystallite size. This observation could be explained that the size of the final particle much depend on the size of the droplets in the emulsion core which were influenced by the water content [53]. At high water content, there are more free water molecules in CEAs resulting in the interfacial rigidity is poorer as compared with at lower water content. These lead to enhance the exchange rate of reactants among micelles and widen the particle size distribution. So, it could be rationalized that the presence of free water in the CEAs provides morphological tailoring of particles [52].

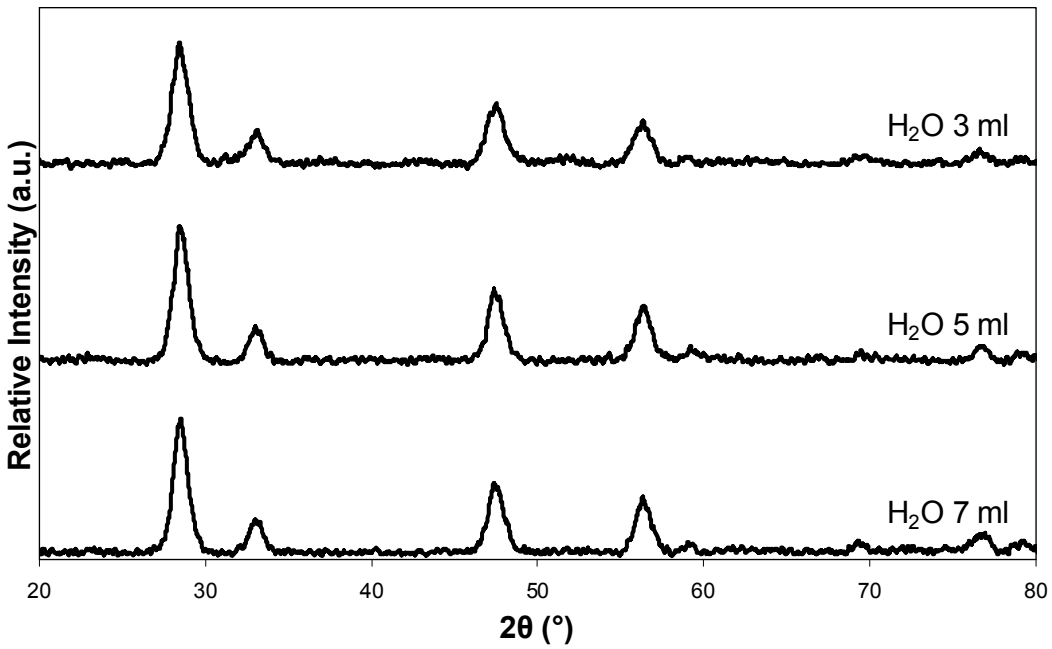

Figure 4.16 XRD patterns of CeO_2 prepared by CEAs method at different water content.

Table 4.6 Surface area, porosity, crystallite size and percent yield of CeO_2 prepared by different water content.

Water content (ml)	Surface area (m^2/g)	Pore volume (cm^3/g)	Pore size (Å)	Crystallite size (nm)	%Yield
3	145.73	0.2170	59.5	5.81	84.29
5	102.9	0.2174	84.5	5.91	84.47
7	94.5	0.1804	76.4	6.45	87.78

4.6 Summary

Nano-sized CeO_2 was successfully prepared by different microemulsion methods. The results from XRD, TEM and BET measurement indicated that the obtained particles were cubic fluorite structure CeO_2 nanoparticles. All the methods used the colloidal system as synthesis media as this media can control synthesis to manipulate the particle size, morphology and size distribution. As a result, the particles obtained in such a medium are generally very fine and have a narrow size distribution. The preparation by colloidal emulsion aphrons method using $(NH_4)_2Ce(NO_3)_6$ as a cerium source, PE4LE as a surfactant and three milliliter of water content was chosen as the suitable condition for produced nano-sized CeO_2 with the highest surface area and the smallest particle size. The surface tensions of cerium solution have slightly effect on the particle size. The hydrocarbon chain lengths of nonionic surfactant have affection of solubility in emulsion and could be decrease in particle size. A mutual repulsion between hydrophilic group of the cationic surfactant and nanoparticle surface might be weaker, as a result, CeO_2 particles became larger than that used nonionic surfactant. Calcinations in higher temperature make the average size of products increasing. By increasing the water content the final particle of CeO_2 was increased.